Analyst

Accepted Manuscript

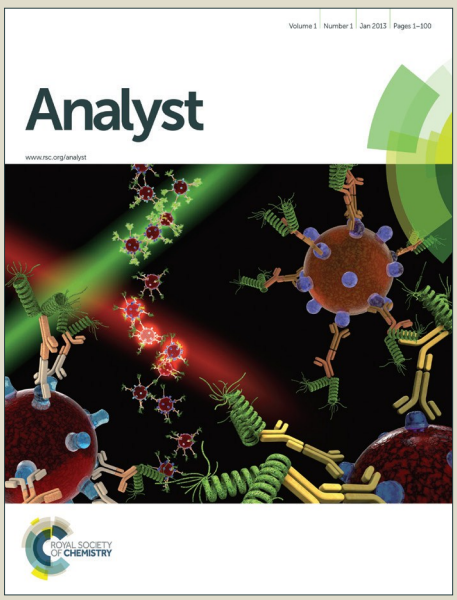

ROYAL SOCIETY OF CHEMISTRY

www.rsc.org/analyst

Full paper

A colorimetric probe to determine Pb^{2+} using functionalized silver nanoparticles

Kwon-Chul Noh,[a,b,†] Yun-Sik Nam,[a,†] Ho-Jin Lee[a] and Kang-Bong Lee[a,*]

[a]*Advanced Analysis Center and Green City Technology Institute,*

Korea Institute of Science and Technology

P.O. Box 131, Cheongryangri, Seoul 130-650, Republic of Korea

[b]*Department of Chemistry, Korea University*

P.O. Box 145, Anam-ro, Seongbuk-gu, Seoul 136-701, Republic of Korea

[*]Corresponding author. Tel.: +82 2 958 5957; fax.: +82 2 958 5810

E-mail address: leekb@kist.re.kr (K.-B. Lee).

[†] These authors contributed equally to this work.

A simple and sensitive colorimetric method for the determination of Pb^{2+} ions in aqueous samples was developed using 1-(2-mercaptoethyl)-1, 3, 5-triazinane-2, 4, 6-trione (MTT) functionalized silver nanoparticles (MTT–AgNPs). The Pb^{2+} ion acted as the metal center of the coordination complex, which formed N---Pb^{2+}---O coordination bonds with the MTT–AgNPs, shortening the interparticle distance, and inducing aggregation of the MTT–AgNPs. This aggregation resulted in a dramatic color change from yellow to dark blue. Using this methodology, the concentration of Pb^{2+} ions in environmental samples could be quantitatively detected by the naked eye or by using UV–vis spectrometry. Also, we found that the selectivity and sensitivity of the detection was noticeably improved at the pH range 7-8, at which a more obvious color change was observed. The absorption ratios (A_{625}/A_{395}) of the modified AgNPs solution exhibited a linear correlation with Pb^{2+} ion concentrations within the linear range of 0.1~0.6 μg/mL, and the limits of detection in tap and pond water were 0.02 and 0.06 μg/mL, respectively. This cost-effective sensing system allows for the rapid and facile determination of Pb^{2+} ions in aqueous samples.

Keywords: Pb^{2+} ion; silver nanoparticles; 1-(2-mercaptoethyl)-1, 3, 5-triazinane-2, 4, 6-trione; colorimetric detection

Introduction

Lead ions (Pb^{2+}) are highly toxic heavy-metal ions that can cause serious environmental and health problems and are ubiquitous in industry.[1,2] Extensive studies have indicated that humans, especially children, can suffer permanent neurological damage and behavioral dysfunction when exhibiting even low blood levels of lead.[3] To date, no safe lead-exposure threshold has been identified. The ability of lead to pass through the blood-brain barrier is largely due to its ability to act as a substitute for calcium ions.[4] Within the brain, lead-induced damage in the prefrontal cerebral cortex, hippocampus, and cerebellum can lead to a variety of neurologic disorders. At the molecular level, lead ions interfere with the regulatory action of calcium on cell function and disrupt a range of intracellular biological activities.[5] Therefore, facile methods to monitor Pb^{2+} levels in the environment are of increasing importance and a sensitive method for routinely and effectively measuring the concentration of Pb^{2+} is crucial in environmental monitoring.

To date, a variety of analytical methods have been reported for the determination of Pb^{2+} ions including atomic absorption spectrometry (AAS),[6–8] inductively coupled plasma mass spectrometry (ICP–MS),[9,10] and fluorescence[11,12] and electrochemical[13] methods. However, most of these methods require complex instrumentation and well-trained operators. Hence, development of an accurate, rapid, and convenient analytical method to detect Pb^{2+} ions remains a challenge for analytical chemists.

With developments in nanotechnology, novel colorimetric assays for Pb^{2+} ions using gold and silver nanoparticles (AuNPs and AgNPs, respectively), have been developed. These methods exploit sensing receptors for nanoparticles coordinated to Pb^{2+} ions. These Pb^{2+}-coordinated functionalized nanoparticles possess unique size-dependent and interparticle distance-dependent optical properties with accompanying color changes. In recent years, AuNP- and AgNP-based colorimetric methods using nanoparticle that are functionalized with ligands of appropriate specificity and affinity for Pb^{2+} ions have been reported. For example, Lu *et al.* reported the construction of a Pb^{2+} biosensor using a DNAzyme-directed assembly of AuNPs[14–16] and Thomas *et al.* showed that AuNPs functionalized with gallic acid were sensitive to Pb^{2+} ions in aqueous media.[17] In addition, Jiang *et al.* and Wang *et al.* reported that AuNPs functionalized with peptide derivatives can serve as Pb^{2+} color sensors.[18–20]

When the surface of the AuNP is coated with a loose layer of citrate, its carboxyl groups have a strong and

selective affinity for Pb^{2+} ions at high pH values.[21] Therefore, both the sensitivity and selectivity of the AuNPs for heavy metal ion detection are dependent on the pH of the environments. Additionally, AgNPs functionalized with amino acids or plant extracts have been utilized to detect Pb^{2+} simultaneously with $Hg^{2+}$and Cd^{2+} ions.[22,23] Lu *et al.* and Lee *et al.*[24,25] have developed 1-(2-mercaptoethyl)-1,3,5-triazinane-2,4,6-trione (MTT)-stabilized AuNPs as a colorimetric probe for melamine detection in milk and NO_2^- ion monitoring in aqueous solution, by utilizing their hydrogen-bonding interactions with MTT.

Informed by these studies, we have examined the application of AgNPs functionalized with MTT as a novel and sensitive probe for the determination of metal ions in aqueous samples, because the N and O atoms of the MTT molecules at a specific pH coordinate to metal ions. In addition, MTT can be easily conjugated to AgNPs through the -SH group in the same way as it can to AuNPs (Fig. 1).

We found that MTT–AgNPs respond to Pb^{2+} with a more obvious color change than that observed with other metal ions, including Li^+, Cd^{2+}, Co^{2+}, Na^+, Ba^{2+}, Ni^{2+}, Ca^{2+}, Mg^{2+}, K^+, As^{3+}, Ti^{3+}, Ga^{3+}, Hg^{2+}, Ge^{4+}, Zn^{2+}, and Cr^{3+}. Moreover, the AgNPs-based system exhibited better sensitivity for the detection of Pb^{2+} ions in neutral pH solution. The absorption ratio (A_{625}/A_{395}) of the modified AgNPs in the pH-optimized system exhibits a linear correlation over Pb^{2+} ion concentration range of 0.1~0.6 μg/mL, allowing the determination of Pb^{2+} ion concentration in aqueous samples within three minutes. Therefore, we suggest that an optimized MTT–AgNP system can be used as a facile and low-cost sensor for on-site and real-time Pb^{2+} ion detection. This technique could have a wide range of practical applications.

Experimental

Materials

Silver(I) nitrate, sodium borohydride, ethyl chloroformate, acetone, and potassium thiocyanate were from Sigma-Aldrich (St. Louis, MO, USA). Methylene chloride and HCl were obtained from J. T. Baker (Phillipsburg, NJ, USA). The salts of the metal cations-Pb^{2+}, Li^+, Cd^{2+}, Co^{2+}, Na^+, Ba^{2+}, Ni^{2+}, Ca^{2+}, Mg^{2+}, K^+, As^{3+}, Ti^{3+}, Ga^{3+}, Hg^{2+}, Ge^{4+}, Zn^{2+}, and Cr^{3+} were from Accu Standard (New Haven, CT, USA). pH paper was obtained from Whatman International Ltd. (Maidstone, UK). HCl and NaOH were obtained from Samchun Chemical (Gyeong gi-Do, Korea). Distilled water used in this work was obtained through a Milli-Q water

purification system from Millipore (Bedford, MA, USA).

Apparatus

The absorption spectra of the AgNPs were recorded at room temperature using an S–3100 UV–vis spectrophotometer S–3100 (Sinco, Seoul, Republic of Korea). UV–vis spectra were measured in the range of 300–800 nm using quartz cells of 1 mm path length. pH measurement was performed on a HI 2210 pH meter (Hanna Instruments, Woonsocket, RI, USA). All IR spectra were measured using an FT-IR spectrometer (Thermo Mattson, Infinity Gold FT-IR, Waltham, MA, USA) equipped with a mercury cadmium telluride detector and a zinc selenide crystal attenuated total reflection device. Particle size distributions were measured using a Zetasizer (Malvern Instruments Ltd., Worcestershire, UK). The image and the diameter of the MTT–AgNPs and the Pb^{2+}-induced aggregation of MTT–AgNPs were measured from a micrograph using a CM30 transmission electron microscope (TEM) (Philips, NC, USA). TEM specimens were obtained by depositing a dispersion of the AgNPs and evaporating the solvent. The concentrations of Pb^{2+} in aqueous solutions were measured using atomic absorption spectrometry (AAS) (Varian Inc., Palo Alto, CA, USA).

Preparation of MTT and AgNPs conjugated with MTT

MTT was synthesized according to a literature procedure,[26] and MTT-conjugated AgNPs were then prepared by a ligand-exchange reaction between MTT and borohydride-stabilized AgNPs. We synthesized ca. 10 nm AgNPs by the reduction of silver nitrate using sodium borohydride. Typically, 25 mL of 1 mM silver nitrate was added dropwise to 150 mL of 2 mM sodium borohydride solution chilled in an ice bath. The reaction mixture was stirred for a total of 6 h under a nitrogen atmosphere (3 h) and air (3 h), and light yellow nanoparticles were obtained. The ligand-exchange reaction was performed at room temperature by mixing 1 mL of the prepared silver colloid with 1 mL of aqueous 0.1 mM MTT under stirring. 0~70 μL volumes of 0.1 mM MTT were added to 1 mL of AgNPs to investigate their self-aggregation. No color change was observed in the MTT–AgNP solution formed with the addition of MTT, which indicated that no self-aggregation of the MTT–AgNPs has occurred.

Colorimetric detection of Pb^{2+}

To evaluate the utility of our proposed method, the Pb^{2+} concentration in tap and pond water was quantified. Tap water samples were obtained from our lab and pond water samples were obtained from a pond in our research institute. Our method was validated using AAS. Prior to analysis, all samples were filtered using a syringe filter (0.20 μm pore size) to remove suspended particles, and 9 mL of the sample was mixed with 1 mL of 100 μg/mL Pb^{2+} to make a 10 μg/mL Pb^{2+} stock solution. Approximately 0 – 10 μL of real water samples containing 0 – 1.0 μg/mL of Pb^{2+} were added to 1 mL MTT–AgNPs, which were then analyzed by UV–vis spectrophotometry.

Results and discussion

AgNPs strongly absorb light in the visible region, where the frequency of the incident electromagnetic field is resonant with the coherent oscillation of the electrons on the surface of the nanoparticles. This phenomenon is called localized surface plasmon resonance (LSPR). A strong LSPR absorption peak appears at ca. 395 nm in the UV–vis spectra of AgNPs, which results in AgNPs displaying a yellow color in solution (Fig. 1A). The LSPR peak frequency is influenced by the size and shape of the nanoparticles, the refractive index of the surrounding medium, and the degree of aggregation.[27–29]

Selectivity of MTT-Functionalized AgNPs for Pb^{2+} ions

We synthesized MTT, a thiol-functionalized cyanuric acid,[26] and prepared ca. 10 nm MTT–AgNPs using the ligand-exchange reaction of AgNPs with MTT. The AgNPs size under these preparation conditions is much smaller than that of the MTT-stabilized AuNPs synthesized in an earlier study (ca. 33 nm).[25] The mean size of the AgNPs was dependent upon the amount of sodium borohydride used and other preparation conditions. It is known that the AgNPs size affects the surface plasma absorption maxima.

The AgNPs conjugated with MTT were well dispersed with a mean size of 10 nm and displayed a uniform yellow color due to the strong LSPR at 395 nm. We hypothesized that MTT-AgNPs may be developed as a simple colorimetric assay for the selective detection of metal ions. We found that addition of 0.4 μg/mL Pb^{2+} to MTT-AgNPs solutions rapidly induces color change from yellow to dark blue, due to the Pb^{2+} binding with MTT and the decreasing distance between AgNPs. The UV-vis absorption spectrum of MTT-AgNPs in the presence of Pb^{2+} ions shows that the absorption band at 395 nm decreases and a new absorbance band at 625 nm

increases (Fig. 1A). The absorption band at 625 nm could be attributed to coupled plasmon absorbance, caused by contact with other nanoparticles due to the aggregation of AgNPs.

The selectivity of MTT-AgNPs sensors was also investigated using numerous metal ions, including Li^{+}, Cd^{2+}, Co^{2+}, Na^{+}, Ba^{2+}, Ni^{2+}, Ca^{2+}, Mg^{2+}, K^{+}, As^{3+}, Ti^{3+}, Ga^{3+}, Hg^{2+}, Ge^{4+}, Zn^{2+}, and Cr^{3+} at a concentration of 0.4 μg/mL. We observed that these metal ions induced a minor color change from light yellow to dark yellow (Fig. 1B). The UV–vis absorption spectra of the MTT–AgNPs solutions in the presence of other metal ions were also obtained (Fig. 1C), and the strong absorption band at 625 nm for MTT-AgNPs is notably unique for Pb^{2+} ion and can be differentiated easily from other metal ions.

The selectivity of AgNPs towards various metal ions was further studied by plotting the absorbance of the MTT–AgNP solution in the presence of each metal ion. The selectivity of the optimized sensor for Pb^{2+} ions was evaluated by comparison of the absorbance ratio (A_{625}/A_{395}) with that of solutions containing other metal ions, as shown in Fig. 1D. A higher ratio was attributed to aggregated nanoparticles, which exhibited a sky blue color, whereas a lower ratio indicated that the MTT–AgNPs had dispersed well.[18] It was found that AgNPs conjugated with MTT responded selectively to Pb^{2+} ions, as indicated by the dramatic increase in the absorbance ratio (A_{625}/A_{395}). The absorbance ratio (A_{625}/A_{395}) induced by the Pb^{2+} ion was ca. 6–7-fold greater than those of other metal ions, which indicated the unique interaction between MTT–AgNPs and Pb^{2+} ions.

To further confirm the selectivity of MTT–AgNPs, we tested MTT–AgNP sensors with Pb^{2+} ions in aqueous solution mixed with other metal ions. These metal ions did not interfere with the determination of Pb^{2+} ion concentration in aqueous solution, even when their concentrations were much higher than the Pb^{2+} concentration. This is because metal ions other than Pb^{2+} do not produce an absorption band at 625 nm.

Sensing mechanism of AgNPs for Pb^{2+} ions

Since the well-dispersed MTT–AgNPs are induced to aggregate by the addition of Pb^{2+} through the formation of the MTT–Pb^{2+} complex, we propose a plausible mechanism for the colorimetric sensing of Pb^{2+} ions by AgNPs (Fig. 2A). Fig. 2B shows a hypothetical structure illustrating the coordinate bonds between the N and O atoms of MTT and Pb^{2+} ions. The amide NH was deprotonated at neutral pH, and the carbonyl group seems to undergo resonance, imparting it with a partial negative charge.

The Pb^{2+} ions are more selectively coordinated than the other metal ions because Pb^{2+} is the only dipositive

metal ion which is effective in promoting peptide nitrogen deprotonation,[30] and Pb^{2+} ions can be coordinated by the N and O atoms of MTT with higher affinity than any other metal ion. In addition, Pb^{2+} exhibits a broad range of coordination numbers from 2 to 12, whereas other metal ions are coordinated with fewer ligands because of their rigid coordination geometry.[17] This means that Pb^{2+} ions can be coordinated and aggregated more easily than other metal ions.

To investigate the sensing mechanism of AgNP nanoparticles for Pb^{2+} ions, we obtained IR spectra for AgNPs, MTT, MTT–AgNPs, and Pb^{2+}–MTT–AgNPs (Fig. 3). The IR spectrum of AgNPs does not show any NH and C=O peaks, as expected (Fig. 3A). The IR spectra of free MTT and AgNPs conjugated with MTT show the characteristic NH band at 3210 cm^{-1} and C=O band at 1700 cm^{-1}, as shown in Fig. 3B and 3C, respectively. In the IR spectrum of Pb^{2+}–MTT–AgNPs, the NH peak becomes very broad, and C=O band is almost absent, as shown in Fig. 3D. These changes in the C=O and N-H peaks indicate that the Pb^{2+} ion is coordinated with the N and O atoms of MTT conjugated with AgNPs.

The TEM images and the size distribution of MTT–AgNPs in the absence and presence of Pb^{2+} ions (measured by a Zetasizer instrument) are shown in Fig. 4. Images of the MTT–AgNPs (Fig. 4A) and the Pb^{2+}-induced aggregation of MTT–AgNPs (Fig. 4B) were acquired. The TEM images reveal that the size of each MTT–AgNP and Pb^{2+}–MTT–AgNPs are ca. 10 and 50 nm, respectively (similar to the results obtained from the Zetasizer), and Pb^{2+}–MTT–AgNPs are significantly more aggregated than MTT–AgNPs in the absence of the Pb^{2+} ion, as shown in Fig. 4B. The reason for the band shift and color change in the presence of Pb^{2+} ions is also illustrated by the TEM images. Specifically, surface electrons oscillated by light cannot homogeneously polarize the nanoparticles of small dispersed AgNPs, and higher order modes at lower energies dominate, which can cause a red shift and broadening of the localized surface plasmon band.

Optimization of the sensitivity of the MTT-functionalized AgNP sensor

Since MTT–AgNPs showed selectivity for Pb^{2+}, we examined the stability and sensitivity of the MTT–AgNPs by controlling the relative amount of Pb^{2+}, the pH, and the concentration of MTT.

The performance of the developed Pb^{2+} sensor was strongly influenced by the pH of the solution, because media pH not only influences the interaction between MTT–AgNPs and Pb^{2+} ions, but also affects the stability

of AgNPs (Fig. 2B). We examined the changes in color and absorbance of MTT–AgNPs alone as a function of pH, and there were no changes over the pH range 5-10 (not shown). However, the absorption ratio (A_{625}/A_{395}) for Pb^{2+}–MTT–AgNPs at the pH range 7-8 increase dramatically (see Fig. S1 in the supporting information). This indicates that the coordination bond between MTT and Pb^{2+} is formed more easily at neutral pH. The first pKa of MTT was predicted to be 6.7 (Marvin software, ChemAxon Ltd, Budapest, Hungary),; therefore, we reasoned that MTT was bound through a carbonyl O atom and a deprotonated N atom to Pb^{2+} as the dianionic N,O-bidenate form at neutral pH (The pKa of cyanuric acid is 6.8).[30] The amide NH was deprotonated at neutral pH, and the carbonyl group appears to undergo resonance, which imparts partial negativity to the CO^- moiety. Under more basic conditions, more hydroxyl (OH^-) groups in the solution may interact with the Pb^{2+} ions, which may result in the inhibition of coordination between Pb^{2+} and MTT.[31,32] The pH range 7-8 was suitable for this assay in terms of the sensitivity of MTT–AgNPs towards Pb^{2+} ions, but the selectivity of the method at pH 8 was much better than that of pH 7; we selected pH 8 as the optimum pH.

In addition, various concentrations of MTT in AgNP solutions with a 0.4 μg/mL Pb^{2+} ion concentration were tested, and their UV–vis spectra and absorbance ratios (A_{625}/A_{395}) were monitored to identify the optimum concentration of MTT for AgNP aggregation. We found that the color change of AgNPs in 0.4 μg/mL Pb^{2+} ion concentration was optimized at ca. 30–35 μL of MTT (see Fig. S2 in the supporting information).

The color change induced by Pb^{2+} ions can be monitored by UV–vis spectrometry, and these color changes depend on the concentration of Pb^{2+} ions. The color of the AgNPs changed progressively from yellow to dark blue in accordance with the increase in Pb^{2+} ion concentration, as shown in Fig. 5A. An increase in the absorbance in the 625 nm region and a concomitant decrease in the intensity of the LSPR peak at 395 nm were observed with increasing Pb^{2+} ion concentration (0, 0.1, 0.2, 0.3, 0.4, 0.5, and 0.6 μg/mL) in MTT–AgNP solutions as shown in Fig. 5B. The absorbance ratio (A_{625}/A_{395}) was measured three times at each Pb^{2+} ion concentration for the quantitative analysis of the Pb^{2+} ion, as shown in Fig. 5C. Linear regression analysis of the calibration curve with error bars was performed and good linearity (correlation coefficient, r^2 = 0.992) was obtained within the concentration range of 0.1–0.6 μg/mL in pond water. A limit of detection (LOD) of 0.06 μg/mL [3σ/slope] in pond water was derived for this colorimetric probe, and an LOD of 0.02 μg/mL in tap water

was obtained.

These color changes seem to represent the relative amounts of aggregated and monodispersed AgNPs. We examined the aggregation kinetics of MTT–AgNPs reacting at various Pb^{2+} ion concentrations by monitoring the absorbance ratios ($A_{625}/_{395}$), since a sensor with a fast response at room temperature would be highly desirable for on-site and real-time detection. It was found that a 3 min reaction time was required regardless of the Pb^{2+} ion concentration as shown in Fig. 6.

Application of the MTT-functionalized AgNP sensor in real water samples

In order to validate the present method, we tested its colorimetric response in real water samples. The concentrations (0.3 and 0.5 μg/mL) of Pb^{2+} ions spiked in tap and pond water samples were measured by the MTT–AgNPs colorimetric probe and AAS. As shown in Table 1, the analytical results of the developed colorimetric sensor are similar to those monitored by AAS. Furthermore, the determination of Pb^{2+} ions has been performed with pond water from the garden in our research institute containing complex media. Pb^{2+} was not detected within the LODs (0.06 μg/mL) by either the colorimetric AgNP probe or AAS, as shown in Table 2. Therefore, the use of this colorimetric AgNPs-based probe for the detection of Pb^{2+} ions in aqueous samples could be an improvement on currently used instrumental methods in terms of cost, simplicity, and time.

The sensitivity of this colorimetric sensor was compared to those of earlier methods using nanoparticle sensors (Table 3).[19,20,33–36] Also, we attempted to apply our method to bovine serum to evaluate the possibility of biological application. However, the method was not applicable this situation because Pb^{2+} has a strong affinity to proteins.[37] Thus, this sensor will be solely applied to environmental samples.

Conclusions

In this paper, we developed a novel sensitive and selective sensor for the visual detection of Pb^{2+} by means of the color change associated with AgNP aggregation. This method offers several advantages over the existing Pb^{2+} detection techniques. Firstly, the method does not require expensive or complicated instrumentation, which simplifies operations and reduces the associated costs. Secondly, it allows detection of concentrations as low as

0.02-0.06 μg/mL to be achieved visually within 30 min, resulting in the rapid and sensitive detection of Pb^{2+} ions. Finally, this sensor exhibits excellent selectivity for Pb^{2+} over other metal ions.

Acknowledgements

The authors thank the Korean Ministry of Science, ICT and Future Planning for the financial support for the present research (2N39430, 2E25290, and 2N39960).

Appendix A. Supplementary data

Supplementary data associated with this article can be found, in the online version, at http://

References

1 P. C. Hsu and Y. L. Guo, *Toxicology*, 2002, **180**, 33–44.

2 M. M. Larsen, J. S. Blusztajn, O. Andersen and I. Dahllöf, *J. Environ. Monit.*, 2012, **14**, 2893–2901.

3 T. R. Guilarte, M. Opler and M. Pletnikov, *Neurotoxicology*, 2012, **33**, 560–574.

4 M. Kirberger and J. J. Yang, *J. Inorg. Biochem.*, 2008, **102**, 1901–1909.

5 C. D. Toscano and T. R. Guilarte, *Brain Res. Rev.*, 2005, **49**, 529–554.

6 M. Soylak, A. Kars and I. Narin, *J. Hazard. Mater.*, 2008, **159**, 435–439.

7 L. R. Bravo-Sánchez, B. S. V. Riva, J. M. Costa-Fernández, R. Pereiro and A. Sanz-Medel, *Talanta*, 2001, **55**, 1071–1078.

8 P. Bermejo-Barrera, M. C. Barciela-Alonso, J. Moreda-Piñeiro, C. González-Sixto and A. Bermejo-Barrera,

Spectrochim. Acta Part B At. Spectrosc., 1996, **51**, 1235–1244.

9 L. Xia, X. Li, Y. Wu, B. Hu and R. Chen, *Spectrochim. Acta Part B At. Spectrosc.*, 2008, **63**, 1290–1296.

10 W. H. Hsu, S. J. Jiang and A. C. Sahayam, *Talanta*, 2013, **117**, 268–272.

11 M. Li, X. Zhou, S. Guo and N. Wu, *Biosens. Bioelectron.*, 2013, **43**, 69–74.

12 L. Guo, D. Nie, C. Qiu, Q. Zheng, H. Wu, P. Ye, Y. Hao, F. Fu and G. Chen, *Biosens. Bioelectron.*, 2012, **35**, 123–127.

13 G. P. Jin, S. Y. Xu, P. Lei, Y. Fu, X. Feng, Z. X. Wu, M. Yu, S. Dai and G. Liu, *Electrochim. Acta*, 2014, **130**, 526–531.

14 J. Liu and Y. Lu, *Chem. Mater.*, 2004, **16**, 3231–3238.

15 X. M. Miao, L. S. Ling and X. T. Shuai, *Anal. Biochem.*, 2012, **421**, 582–586.

16 C. H. Chung, J. H. Kim, J. Jung and B. H. Chung, *Biosens. Bioelectron.*, 2013, **41**, 827–832.

17 K. Yoosaf, B. I. Ipe, C. H. Suresh and K. G. Thomas, *J. Phys. Chem. C*, 2007, **111**, 12839–12847.

18 Y. Guo, Z. Wang, W. Qu, H. Shao and X. Jiang, *Biosens. Bioelectron.*, 2011, **26**, 4064–4069.

19 D. Zhu, X. Li, X. Liu, J. Wang and Z. Wang, *Biosens. Bioelectron.*, 2012, **31**, 505–509.

20 F. Chai, C. Wang, T. Wang, L. Li and Z. Su, *ACS Appl. Mater. & Interfaces.*, 2010, **2**, 1466–1470.

21 J. Guan, L. Jiang, L. Zhao, J. Li and W. Yang, *Colloids Surf. A Physicochem. Eng. Asp.*, 2008, **325**, 194–197.

22 V. V. Kumar and S. P. Anthony, *Sens. Actuators B Chem.*, 2014, **191**, 31–36.

23 V. V. Kumar, S. Anbarasan, L. R. Christena, N. SaiSubramanian and S. P. Anthony, *Spectrochim. Acta, A: Mol. Biomol. Spectrosc.*, 2014, **129**, 35–42.

24 K. Ai, Y. Liu and L. Lu, *J. Am. Chem. Soc.*, 2009, **131**, 9496–9497.

25 Y. S. Nam, K. C. Noh, N. K. Kim, Y. Lee, H. K. Park, K. B. Lee, *Talanta*, 2014, **125**, 153–158.26 D. L. Klayman and T. S. Woods, *J. Org. Chem.*, 1974, **39**, 1819–1823.

27 S. Link and M. A. El-Sayed, *Int. Rev. Phys. Chem.*, 2000, **19**, 409–453.

28 S. Eustis and M. A. El-Sayed, *Chem. Soc. Rev.*, 2006, **35**, 209–217.

29 P. K. Jain, K. S. Lee, I. H. El-Sayed and M. A. El-Sayed, *J. Phys. Chem. B*, 2006, **110**, 7238–7248.

30 G. Battistuzzi , M. Borsari , L. Menabue , M. Saladini and M. Sola, *Inorg. Chem.*., 1996, **35**, 4239–4247.

31 I. Persson, K. Lyczko, D. Lundberg, L. Eriksson and A. Placzek, *Inorg. Chem*., 2011, **50**, 1058–1072.

32 Y. Guo, Z. Wang, W. Qu, H. Shao and Xingyu Jiang, *Biosens. Bioelectron.,* 2011, **26**, 4064–4069.

33 S. Wu, N. Duan, Z. Shi, C. Fang and Z. Wang, *Talanta*, 2014, **128**, 327–336.

34 M. Annadhasan, T. Muthukumarasamyvel, V. R. Sankar Babu and N. Rajendiran, *ACS Sustainable Chem. Eng.*, 2014, **2**, 887–896.

35 L. Zhang, Y. Yao, J. Shan and H. Li, *Nanotechnology*, 2011, **15**, 275504

36 C. Zhang, L. Huidong, C. Lin, L. Chenbin and L. Shenglian, *J. Nanosci. Nanotech*., 2015, **15**, 1480–1485.

37 A. Belatik, S. Hotchandani, R. Carpentier and H.-A. Tajmir-Riahi, *PLoS ONE*, 2012, **7**, e36723

Table 1. Concentrations of Pb^{2+} ion spiked in tap and pond water samples measured by the MTT–AgNP colorimetric probe and AAS.

Content of Pb^{2+} ion added to tap and pond water samples (n = 6)						
		Colorimetric probe				AAS
Sample	Added amount (μg/mL)	Detected amount (μg/mL)	Coefficient of Variation (%)	Recovery (%)	LOD (μg/mL)	Detected amount (μg/mL)
Tap water	0.3	0.29 ± 0.01	3.9	98.8 ± 3.91	0.02	0.30 ± 0.01
	0.5	0.51 ± 0.01	1.7	100 ± 1.75		0.50 ± 0.01
Pond water	0.3	0.27 ± 0.01	3.8	90.1 ± 3.49	0.06	0.29 ± 0.01
	0.5	0.51 ± 0.03	5.0	101 ± 8.50		0.50 ± 0.02

Table 2. Analytical results for the detection of Pb^{2+} in real water samples obtained from a pond located at Korean Institute of Science and Technology.

	Content of Pb^{2+} ion (μg/mL)	
Sample	Colorimetric probe	AAS
Pond water	< 0.06	< 0.1

Table 3. Comparison of nanoparticle-type sensors proposed for detection of Pb^{2+} in the literature

Analytical technique	Sample matrix	Nanoparticles type	LDR[a]	LOD[b]	Ref.
Colorimetric	Lake water sample	AuNPs	0.1–10 μM	100 nM	20
Colorimetric	Cell	AuNPs	1–10 μM	1 μM	19
FRET[c]	Shrimp or fish	AuNPs-aptamer-bsed	0.1–100 nM	50 pM	33
Colorimetric	Tap&Drinking water	AuNPs	16 –100 μM	16 nM	34
DLS[d]	Drinking water	AgNPs	0.25 pM–0.25 μM	0.25 pM	35
Colorimetric	Lake water	AgNPs	0.5 – 4 μM	0.5 μM	36
This method -colorimetric	Tap & Pond water	AgNPs	1.2-7.3 μM	96.5 nM(Tap water) 289 nM(Pond water)	This study

[a] LDR: Linear dynamic range
[b] LOD: Limit of detection
[c] FRET: Fluorescence Resonance Energy Transfer
[d] DLS: Dynamic Light Scattering

Figure Captions

Fig. 1 (A) Visual colors and UV–Vis spectra of aqueous AgNP (a), MTT–AgNP (b), and Pb^{2+}–MTT–AgNP (c) solutions upon addition of 0.4 μg/mL Pb^{2+}. (B) Visual color change of the MTT-stabilized AgNPs upon addition of 0.4 μg/mL metallic ions (Pb^{2+}, Li^{+}, Cd^{2+}, Co^{2+}, Na^{+}, Ba^{2+}, Ni^{2+}, Ca^{2+}, Mg^{2+}, K^{+}, As^{3+}, Ti^{3+}, Ga^{3+}, Hg^{2+}, Ge^{4+}, Zn^{2+}, or Cr^{3+} ions). (C) UV-vis absorption spectra of the MTT-stabilized AgNPs upon addition of 0.4 μg/mL metallic ions. (D) The corresponding absorbance ratios (A_{625}/A_{395}) in the various metallic ions including the Pb^{2+} ion.

Fig. 2 (A) Schematic diagram of the aggregation of MTT–AgNPs reacted with the Pb^{2+} ion and the associated color change. (B) A hypothetical coordination bond between Pb^{2+} ions and MTT bound to a AgNP.

Fig. 3 FT-IR spectra of (A) AgNPs, (B) MTT, (C) MTT–AgNPs, and (D) Pb^{2+}–MTT–AgNPs.

Fig. 4 (A) TEM image and size distribution of MTT–AgNPs in the absence of Pb^{2+} ions. The mean diameter of MTT–AgNPs is ca. 10 nm. (B) TEM image and size distribution of MTT–AgNPs in the presence of Pb^{2+} ions. The mean diameter of MTT–AgNPs is increased to ca. 50 nm by aggregation.

Fig. 5 (A) Color change of AgNPs functionalized with 1 mM MTT solution upon addition of five different concentrations of Pb^{2+} ions under the optimized conditions. (B) UV-Vis absorption spectra of AgNPs functionalized with 1 mM MTT at a Pb^{2+} ion concentration of ca. 0.1-0.6 μg/mL. (C) The corresponding A_{625}/A_{395} ratios in the UV-Vis absorption spectra of MTT-AgNPs as a function of the Pb^{2+} ion concentration ($y = 1.617x - 0.125$, $r^2 = 0.992$).

Fig. 6 Plots of the time-dependent absorption ratio (A_{625}/A_{395}) over 15 min in the presence of varying concentrations of Pb^{2+} ions.

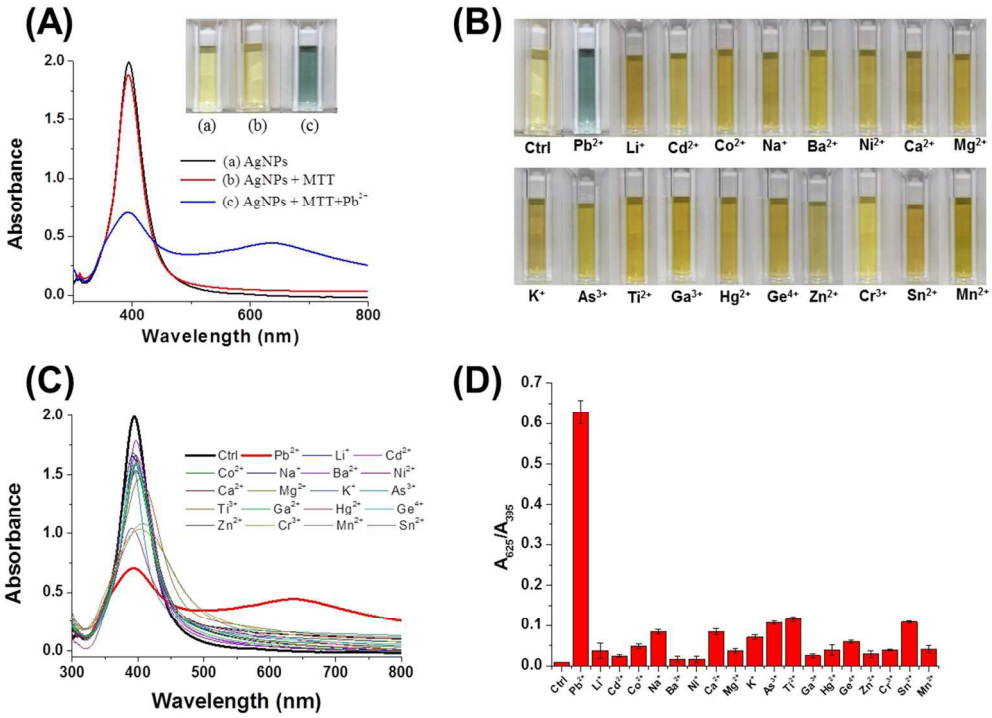

140x101mm (300 x 300 DPI)

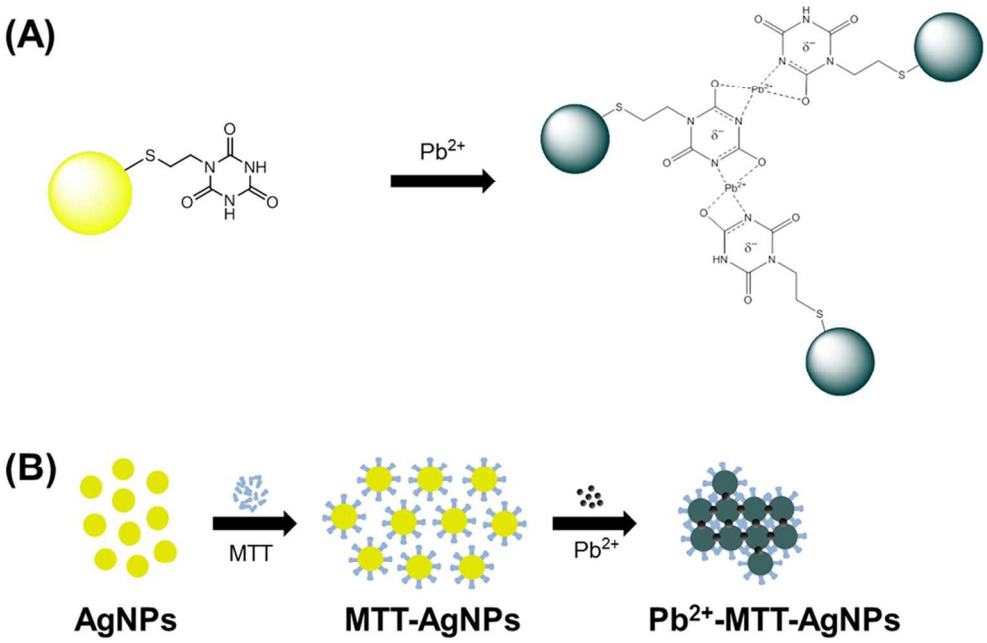

99x66mm (300 x 300 DPI)

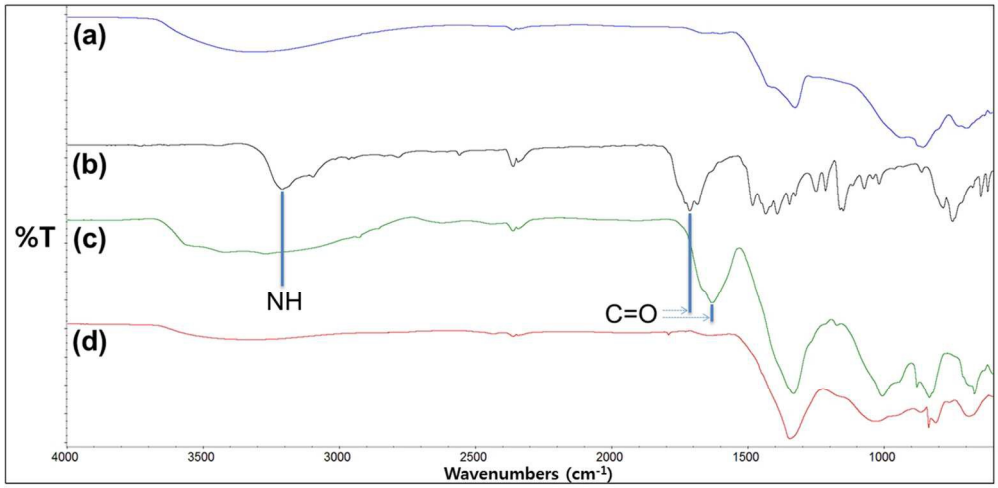

119x58mm (300 x 300 DPI)

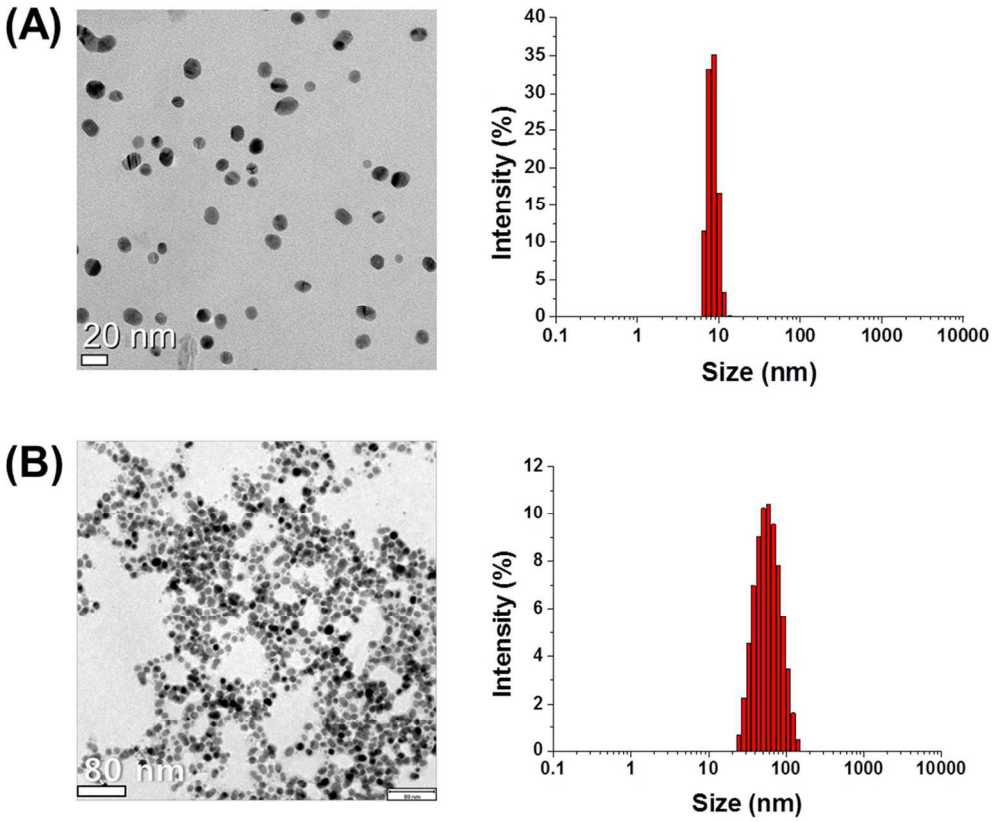

129x107mm (300 x 300 DPI)

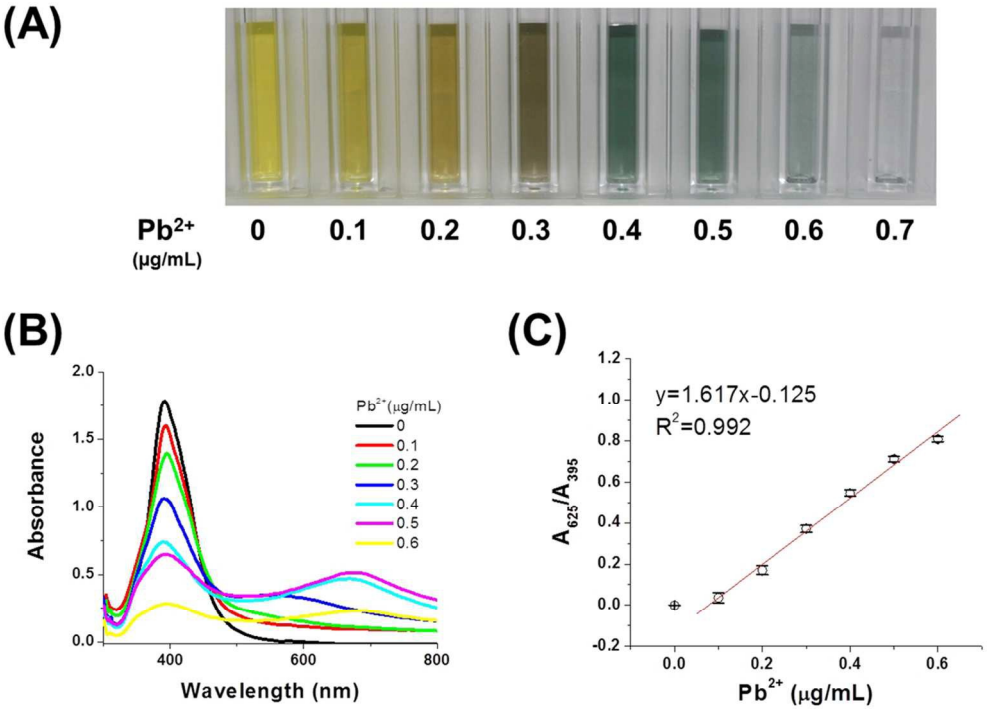

140x100mm (300 x 300 DPI)

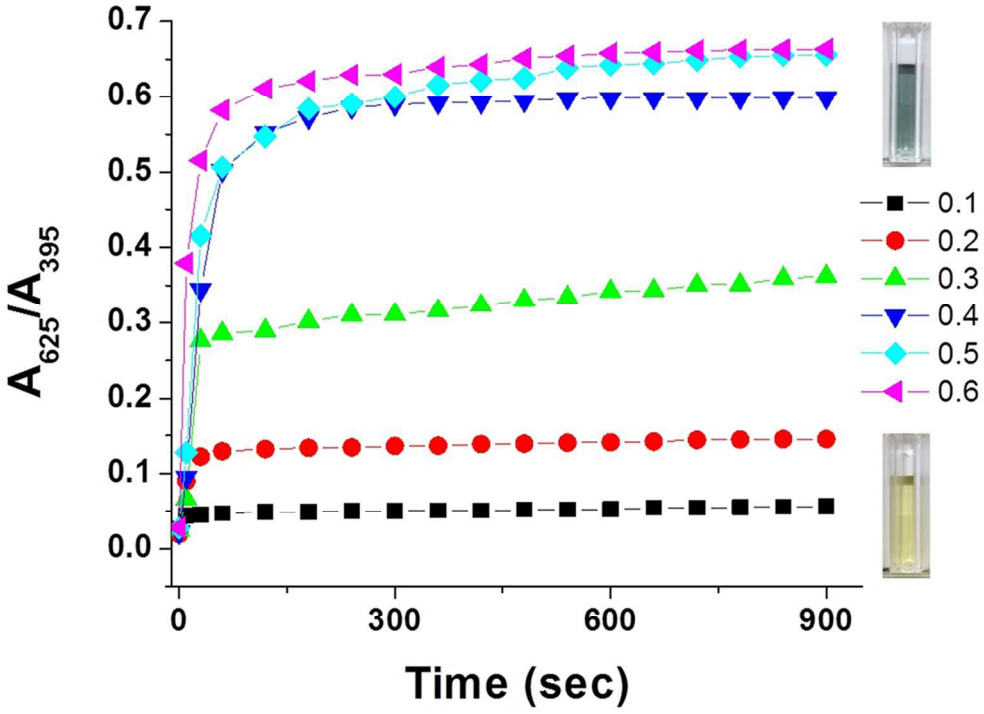

99x72mm (300 x 300 DPI)